A thorny question: the taxonomic identity of the Pirro Nord vertebrae

A thorny question: The taxonomic identity of the Pirro Nord cervical vertebrae revisited

David M. Alba a, b, *, Simone Colombero b, Massimo Delfino b, a, Bienvenido Martínez-Navarro c, Marco Pavia b, Lorenzo Rook d

a Institut Catal_a de Paleontologia Miquel Crusafont, Universitat Aut_onoma de Barcelona, Edifici Z (ICTA-ICP), Carrer de les Columnes s/n, Campus de la UAB,
08193 Cerdanyola del Vall_es, Barcelona, Spain
b Dipartimento di Scienze della Terra, Universit_a di Torino, Via Valperga Caluso 35, 10125 Torino, Italy
c ICREA at Institut Catal_a de Paleoecologia Humana i Evoluci_o SocialeIPHES and _Area de Prehist_oria, Universitat Rovira i Virgili, c/ Marcel·lí Domingo s/n, Campus Sescelades, 43007 Tarragona, Spain
d Dipartimento di Scienze della Terra, Universit_a di Fierenze, Via G. La Pira 4, 50121 Firenze, Italy

* Corresponding author.
E-mail addresses: david.alba@icp.cat (D.M. Alba), simone.colombero@unito.it (S. Colombero), massimo.delfino@unito.it (M. Delfino), bienvenido.martinez@ icrea.cat (B. Martínez-Navarro), marco.pavia@unito.it (M. Pavia), lorenzo.rook@ unifi.it (L. Rook).

Abstract

The past geographic distribution of the genus Theropithecus (Primates: Cercopithecidae) is mainly restricted to Africa. Outside that continent, the earliest reported records of this genus consist of a

calcaneus of cf. Theropithecus sp. from ‘Ubeidiya (Israel, 1.6e1.2 Ma [millions of years ago]), as well as three associated cervical vertebrae from Pirro Nord (Italy, 1.7e1.3 Ma) attributed to Theropithecus sp. The attribution of the Pirro Nord vertebrae to this genus has been disputed on morphometric grounds, although their assignment to a large-bodied cercopithecid has remained undisputed. Here we report unpublished cervical vertebral specimens with a similar morphology and, given their significance for the paleobiogeography of Theropithecus (purportedly representing its earliest European record), we reevaluate their taxonomic attribution. In particular, we reconsider the possibility that they belong to another non-primate mammal recorded at this site. Based on both qualitative and metric morphological comparisons, we strongly favor an alternative attribution of the cervical vertebrae from Pirro Nord to the large porcupine Hystrix refossa, which is widely documented at the site by both dentognathic and other postcranial remains. We therefore conclude that the dispersal of Theropithecus out of Africa before ca. 1 Ma (when it is recorded by dental remains from Cueva Victoria, Spain) is currently based only on the calcaneus from ‘Ubeidiya tentatively attributed to this genus.

Keywords: Vertebrae, Theropithecus, Hystrix, Fossil porcupines, Early Pleistocene, Italy

Introduction

The genus Theropithecus outside Africa The medium to large-sized papionin genus Theropithecus includes a single extant species (Theropithecus gelada) as well as several extinct representatives that are mainly distributed in Africa (Delson, 1993; Pickford, 1993; Jablonski, 2002; Jablonski and Frost, 2010; Gilbert, 2013). The scarce record of this genus outside Africa has therefore received remarkable attention (Hughes et al., 2008; Roberts et al., 2014). Theropithecus is recorded by dental material attributed to Theropithecus oswaldi from both Europe (Cueva Victoria, Spain, ca. 1.0 Ma [millions of years ago]; Gibert et al., 1995) and Asia (Mirzapur, India, ca. 1.0e0.1 Ma; Gupta and

Sahni, 1981; Delson, 1993; Pickford, 1993), as well as by a lower molar of T. cf. gelada from India (Charnel House Cave, > 74 ka [thousands of years ago]; Roberts et al., 2014). A phalanx from Cueva Victoria has also been assigned to Theropithecus (Martínez-Navarro et al., 2005, 2008), and although such an attribution is not universally accepted (e.g., Gibert et al., 2008), this cercopithecid taxon is confidently recorded there by the presence of dental material (Gibert et al., 1995). In contrast, two older records of this genus from Eurasia remain doubtful because they are based on scarce postcranial material. First, an isolated talus from the locality of 'Ubeidiya (Israel, 1.6e1.2 Ma; Martínez-Navarro et al., 2012) has been tentatively attributed to cf. Theropithecus (Belmaker, 2010), because it is impossible to exclude an assignment to another largebodied extinct cercopithecid. Second, three associated cervical vertebrae from Pirro Nord (Italy, 1.7e1.3 Ma) were attributed to Theropithecus sp. by Rook et al. (2004). However, such an assignment has subsequently been disputed by other authors on the basis that these specimens do not provide enough information to warrant an attribution to genus (Frost and Alemseged, 2007; Patel et al., 2007).

The cervical vertebrae from Pirro Nord The associated cervical vertebrae from Pirro Nord (PN34/1, PN34/2, PN34/3, from the fissure identified as PN 34) were attributed to vertebral levels C3, C5 and C6 by Rook et al. (2004). Given the scarcity of fossil vertebrae of Theropithecus, Rook et al. (2004) focused their comparisons on extant large-bodied papionins (Papio, Mandrillus and Theropithecus), macaques (Macaca) and colobines (Colobus and Semnopithecus). These authors argued that morphological similarities, coupled with the known chronological ranges of other large-bodied fossil cercopithecids, justified an attribution to Theropithecus sp. (Rook et al., 2004; Rook, 2009; Rook and Martínez-Navarro, 2013). Given the lack of dental remains, they refrained from providing an identification to the species level, merely noting that the Pirro Nord vertebrae were congruent in size with T. oswaldi. Subsequently, Patel et al. (2007) studied a much larger sample of extant cercopithecid cervical vertebrae by means of discriminant analyses, which showed that this anatomical region provides a poor taxonomic discrimination (based on their linear measurements) at

the genus level in this primate sample. Accordingly, they concluded that the Pirro Nord vertebrae could not be attributed confidently to Theropithecus, since they displayed “a mixed morphology that is not particularly similar to any single extant cercopithecoid species” (Patel et al., 2007:114). After Rook et al.'s (2004) publication, subsequent excavations at Pirro Nord led to the recovery of additional cervical vertebrae with similar morphology to those originally reported from PN 34, but no craniodental or other postcranial remains attributable to a cercopithecid. Although fossil monkeys are usually scarce, the sole preservation of cervical vertebrae would be a strange taphonomic bias, which made us reconsider the possibility that the Pirro Nord vertebrae might be non-primate. In fact, Patel et al. (2007:114) explicitly considered “whether these vertebrae belong to a primate at all” and took into account the alternative possibility that “they may belong to some othermammal found at the site.” Consequently, they compared the Pirro Nord vertebraewith those of various extant carnivorans and ungulates, leading them to conclude that the Pirro Nord vertebrae were most likely cercopithecid instead of non-primate. Unfortunately, Patel et al. (2007) did not evaluate the possibility that these specimens might belong to the porcupine Hystrix refossa, which is a relatively common taxon at Pirro Nord (Rook and Sardella, 2005, 2013; Pavia et al., 2012). In this regard, it is noteworthy that Rook and Sardella (2005) described more than 50 specimens of this extinct species of porcupine fromthis site, including dentognathic as well as postcranial remains (humerus, radius, ulna, femur, tibia, talus, calcaneus and metapodials), but no vertebrae. With an estimated age between 1.7 and 1.3 Ma (Rook et al., 2004; Arzarello et al., 2007, 2009, 2012; Pavia et al., 2012), the Pirro Nord vertebrae might represent the oldest record of Theropithecus in Eurasia. Given their significance for the paleobiogeography of this primate genus, here we re-evaluate the taxonomic affinities of PN 34/1e3 by means of both qualitative and quantitative morphological comparisons between Theropithecus and Hystrix cervical vertebrae.

Materials and methods

Studied sample

Fossil specimens The three cervical vertebrae (PN34/1, PN34/2, PN34/3) from Pirro Nord described by Rook et al. (2004) are temporarily housed in the Earth Sciences Department (University of Florence, Italy). Other cervical vertebrae (other than atlas and axis) from Pirro Nord showing a similar morphology (MGPT-PU 104795, MGPT-PU 104796, MGPT-PU 104797, MGPT-PU 126233, MGPT-PU 126234 and MGPT-PU 126716) are housed in the Museo di Geologia e Paleontologia, Universit_a di Torino (Turin, Italy). Other specimens from Pirro Nord that might belong to other vertebral regions of the same taxon were excluded from study.

Extant comparative sample The fossil specimens mentioned above were compared with cervical vertebrae of T. gelada (Primates, Cercopithecidae; N ¼ 3 individuals) and three extant porcupine species (Hystrix cristata, Hystrix indica and Hystrix africaeaustralis; N ¼ 8 individuals), housed in the Department of Mammalogy of the American Museum of Natural History (AMNH, New York, USA).

Published descriptions of hystricid vertebrae (Yilmaz, 1998; Lopez, 2013, Figs. 5e11) are too succinct for the purposes of this paper. Therefore, most of the morphological details provided here for the cervical vertebral morphology of Hystrix are based on the observations made by one of the authors (D.M.A.), as is the case for those of extant T. gelada.

Morphometric comparisons

We performed canonical discriminant analyses based on the sex-species means of eight metrical variables previously reported by Patel et al. (2007, their Appendix) for a large sample of cercopithecid cervical vertebrae (C3 to C7, including 517 vertebrae from 106 individuals; see Patel et al., 2007, their Table 1, for further details on sample sizes). To these data, we added the mean species values for the Hystrix specimens measured by us. Besides the specimen PN34/2, previously identified by Rook et al. (2004) as a C5 and assigned by us to level C7 (see below), three of the newly reported specimens (MGPT-PU 104795, MGPT-PU 104796 and MGPTPU 104797, respectively a C3 and two C5s) are complete enough to take (or estimate) all of the required measurements (Table 1), enabling their inclusion in the discriminant analyses (see Results for

further details on the preservation of the specimens). Before performing the discriminant analyses, the differences between Theropithecus and Hystrix for all of the included variables separately were inspected by means of boxplots and analysis of variance (ANOVA).

Vertebral measurements were taken with digital calipers to the nearest 0.1 mm, according to the definitions provided by Rook et al. (2004) and Patel et al. (2007, their Table 2 and Fig. 2). Although more individuals of Hystrix spp. were inspected, some of them could not be measured because they were articulated, and among the disarticulated ones only four (three H. cristata and one H. indica) possessed sufficiently well-preserved vertebrae to take all of the required measurements. Following Patel et al. (2007), these measurements were transformed into Mosimann shape variables by dividing them by their geometric mean (Mosimann, 1970; Jungers et al., 1995). Unlike in Patel et al. (2007), in order to maximize taxonomic discrimination and not to assume a priori any vertebral level assignment for the fossil specimens, C3 to C7 measurements were analyzed in the same discriminant analysis, with extant groups being defined on the basis of genus attribution. To avoid the potential confounding effects of differences between different cervical vertebrae and/or cercopithecoid taxa, a second set of discriminant analyses were performed by considering vertebral levels separately (only for those with all the required measurements available in the Pirro Nord sample: C3, C5 and C7) and only distinguishing two groups a priori: cercopithecoid primates and hystricids.

In all of the discriminant analyses, fossil specimens were left ungrouped a priori and classified based on the Mahalanobis squared distance (D2) between the fossil specimens and extant group centroids). For the general discriminant analysis (at the genus level, with all vertebral levels together), we also performed a cluster analysis (Ward's method) based on the centroids for the extant taxa and the discriminant scores of the Pirro Nord vertebrae. Among hierarchical clustering methods, that devised by Ward (1963) intends to select clusters to be fused into larger clusters by minimizing the increase in within-group variance summed over all clusters (Ward, 1963; Hammer and Harper, 2006). Although this method is somewhat biased towards producing clusters with a

similar number of items, it is sensitive to outliers (Milligan, 1980) and it generally performs well, being customarily recommended for morphometric data (Hammer and Harper, 2006). The boxplots and discriminant analyses were performed in SPSS v. 16.0, whereas the cluster analysis was performed using PAST (Hammer et al., 2001).

Body mass estimation

In order to evaluate whether the size of the vertebral specimens described in this paper is consistent with their attribution to the porcupine taxon recorded at Pirro Nord, we estimated the body size of the latter based on the dental measurements published by Rook and Sardella (2013, their Table 1). In particular, body size was estimated based on allometric equations of body mass (in kg) versus both upper and lower tooth row length (in mm), previously published by Freudenthal and Martín-Suarez (2013, their Table 3) for hystricomorph rodents. Following the methodology of these authors for extinct taxa, upper and lower tooth row lengths were computed as the sum of average length values for individual tooth positions. However, given the impossibility of discerning between first and second isolated molars of Hystrix, tooth row lengths were computed as the sum of the average lengths of the fourth premolar, that of the third molar, and twice that of first and second molars together. Correction factors for the logarithmic detransformation bias of 1.14 (upper tooth row) and 1.12 (lower tooth row) were applied, being computed from the standard error of estimates reported by Freudanthal and Martín-Suarez (2013). As recommended by these authors, the final body mass estimate was taken as the average of those delivered by the upper and lower tooth row lengths.

Results

Preservation of the fossil specimens

The three previously-described vertebrae (PN34/1, PN34/2,

PN34/3; Fig. 1f-h) are from a juvenile individual, since they all lack the caudal endplate, and that attributed to level C6 (Fig. 1g) further lacks the cranial endplate. With regard to the newly reported vertebrae (Fig. 1aee,i), several of them also must be from juvenile specimens, as shown by the lack

of the caudal endplate in MGPT-PU 104796 (Fig. 1c) and both the cranial and caudal endplates in MGPT-PU 126716 (Fig. 1e) and MGPT-PU 126234 (Fig. 1i). Only three specimens, MGPT-PU 104795 (Fig. 1a), MGPT-PU 104797 (Fig. 1d), and MGPT-PU 126233 (Fig. 1b) have full epiphyseal fusion and must therefore belong to adult individuals. Furthermore, except for one of the previously-described vertebra (Fig. 1h; PN34/2, here attributed to C7, see below), many of the available specimens are not completely preserved (generally lacking at least part of the transverse and/or spinous processes). Both the incomplete preservation and/or the juvenile condition of the fossil specimens obviously represent a problem for their inclusion in the morphometric analyses. Observations by D.M.A. on the extant comparative sample indicate that non-fused caudal epiphyseal plates are frequently found together with fused cranial epiphyseal plates in subadult individuals otherwise displaying a vertebral size and morphology comparable to fully adult individuals. Accordingly, the only serious problem related to the lack of caudal epiphyseal fusion among the fossil specimens is the concomitant loss of the caudal endplate. Whereas height and width of the body at the caudal endplate can be approximated by that of the remaining portion of the vertebral body, the loss of the endplate results in measurements of ventral length of the body about 10e15% shorter (D.M.A.'s own observations on the comparative sample). Accordingly, this problem was circumvented in the morphometric analyses by dividing such measurements by a correction factor of 0.9 (Table 1). With regard to the broken apex of the spinous process, it precludes taking exact measurements of vertebral height for specimens that otherwise are complete enough to permit taking all of the measurements required by the morphometric analyses. Thus, in a couple of specimens (MGPT-PU 104795 and MGPT-PU 104797), vertebral height was estimated by reconstructing the missing portion of the spinous process (Table 1). Vertebral height can be also estimated in the specimen from PN34/ 3 already attributed by Rook et al. (2004) to a C6, but unfortunately this specimen cannot be included in the morphometric analysis because it lacks both endplates (thereby precluding a reliable estimation of body length). Morphological comparisons Although the cervical vertebrae C3 to C7 of Hystrix and Theropithecus show a superficially similar

morphological pattern, they also display various differences in proportions and morphological details that enable their discrimination (Fig. 2). These are summarized below. Vertebral proportions Irrespective of vertebral level, and relative to overall vertebral size (as approximated by the geometric mean of the various measurements), the cervical vertebrae of Theropithecus are wider (Fig. 3a, b) and taller (Fig. 3c) than those of Hyxtrix, the former further displaying larger (wider and taller) vertebral foramina (Fig. 3d and e) but comparatively smaller (mediolaterally narrower, dorsoventrally lower and craniocaudally shorter) vertebral bodies (Fig. 3feh). In contrast, compared with the distance between the cranial end of the prezygapophyses and the caudal end of the postzygapophyses (not included in the measurements), the vertebral body in Theropithecus appears craniocaudally longer than in Hystrix. Vertebral body In Hystrix, the body displays essentially flat cranial and caudal articular surfaces. In contrast, in Theropithecus the cranial articular surface is markedly concave mediolaterally (especially on its ventral moiety), further markedly protruding cranially on both sides (embracing the sides of the caudal articular surface of the preceding vertebra). Consequently, in Theropithecus the caudal articular surface of each vertebra is neither flat, but somewhat extends onto both sides in cranial direction and also protrudes caudally on its ventral portion. Vertebral arch In Hystrix, the vertebral foramen is subcircular to tunnel-shaped, whereas in Theropithecus it is subtriangular to markedly triangular (especially in C5eC7). Furthermore, the spinous process is stouter and (except in C7) shorter in Hystrix than in Theropithecus. Finally, the articular surfaces between the pre- and postzygapophyses in Hyxtrix are (sub)horizontally oriented (roughly <30_), i.e., the prezygapophyses are only slightly dorsally directed, whereas the postzygapophyses are only somewhat ventrally directed. In contrast, these apophyses in Theropithecus are more vertically oriented (forming an angle of about 45e60_ relative to the main axis of the spine), i.e., the preand postzygapophyses are markedly oriented dorsocranially and ventrocaudally, respectively.

Transverse processes These processes are stouter (taller, longer and generally with more well-developed anterior and posterior tubercles) in Hystrix than in Theropithecus. Moreover, in the

former the transverse processes extend more ventrally and are more caudally directed (at equivalent vertebral levels). In contrast, Theropithecus shows more slender and less caudally directed, but generally more laterally protruding, transverse processes. Transverse foramina In C3eC6, the transverse foramen is clearly wider than it is tall as well as somewhat laterally directed in Theropithecus (so that it can be observed in lateral view), whereas it is rounder and more cranially oriented in Hystrix (not visible in lateral view). The inspected C7 specimens of Theropithecus, unlike those of Hystrix, further lack the transverse foramina. The latter feature, however, might be variable for Theropithecus, as it is for other cercopithecid genera (Schultz, 1961). Attribution of the Pirro Nord specimens Taxonomic attribution Rook et al. (2004) argued that the cervical vertebrae PN34/1, PN34/2, PN34/3 (Fig. 1feh; Table 1) were larger than but similar in morphology to those of extant T. gelada. However, based on the above-mentioned morphological differences between extant Theropithecus and Hystrix (Fig. 2), the Pirro Nord specimens (including those previously described as well as those newly reported here; Fig. 1) much more closely resemble the extant porcupine vertebrae (Figs. 4e8; Table 1). In particular, an attribution of the Pirro Nord vertebrae to Hystrix is supported by the following features: the overall proportions of the vertebrae (which are not markedly wider than tall), the welldeveloped but short vertebral body (shorter than the distance between pre- and postzygapophyses), with flat cranial and caudal articular surfaces, the tunnel-shaped vertebral foramen, the stout and only moderately tall spinous process, the moderate inclination of the pre- and postzygapophyses, the stout and (in some specimens) ventrally well-developed transverse processes, and the transverse foramina invisible in lateral view (and present in C7).

Attribution to cervical vertebral level With regard to anatomical identification, there are some differences from C3 to C7 in Hystrix (Fig. 2) enabling a cervical level assignment for relatively complete isolated fossil vertebrae, such as those from Pirro Nord. Thus, in Hystrix the C3 (Figs. 2b and 4feo) differs from the remaining cervical vertebrae by lacking or merely displaying minimallydeveloped costal processes, as well as by showing very caudallydirected transverse

processes with a restricted development of their ventral portion. From C3 to C5eC6 (Fig. 2b, d, f, h), the costal processes become progressively stouter and more cranially protruding, but also more divergent from the median axis of the vertebra; the spinous process increases in height (especially from C3eC4 to C5eC6), the vertebral foramen becomes taller relative to width, and the pre- and postzygapophyses are consequently situated lower relative to the upper-most portion of the vertebral foramen (at the same level or slightly above the latter in C3eC4, slightly below in C5eC6), the vertebral body becomes progressively taller relative to breadth (especially in C6), and the transverse processes become more transversely (less caudally) oriented as well as more extensive ventrocaudally (especially in C6), and further display a more distinct posterior tubercle (somewhat bifurcated in H. cristata, but not in H. indica). Besides the marked ventrocaudal extension of the transverse processes, the C6 (Fig. 2h) further differs from other cervical vertebra by displaying a more marked ventral keel (which clearly extends until the caudal end of the body). Finally, C7 (Fig. 2j) clearly differs from the preceding cervical vertebrae, because the costal processes lack entirely, the transverse processes are more transversely aligned and lack a ventral extension, the transverse foramina are smaller, the vertebral body is clearly wider than it is tall (unlike in C5eC6, but like in C3eC4), the neural foramen is taller relative to its width, the pre- and postzygapophyses are situated clearly below the upper-most portion of the neural foramen, the spinous process is well developed (at least as tall, if not taller, than in C6), and there are small caudal costal foveae on the most laterocaudal portions of the body. Based on the above-mentioned observations in extant Hystrix and assuming that an attribution to the latter taxon is, as explained above, more likely, it is possible to attribute to cervical vertebral level the new specimens reported here, as well as to re-assess the vertebral level assignments provided by Rook et al. (2004), and accepted by Patel et al. (2007), for the previously-published vertebrae from Pirro Nord (Figs. 4e8). Only a single specimen (MGPT-PU 104795; Figs. 1a and 4pet) is assigned to level C3, based on the lack of costal processes as well as the very caudally-oriented transverse processes with a restricted ventral development. The rather polygonal outline of the cranial endplate (instead of circular or elliptical) further supports an

assignment to C3 instead of C4. This specimen is larger overall than extant Hystrix C3 (Fig. 4f-o), and displays a taller and more caudally-directed spinous process, less dorsally situated pre- and postzygapophyses, and a more elliptical (more wide than tall) caudal endplate, although in other respects it fits well in morphology with porcupine vertebrae from this level. Although the dorsal-most edge of the spinous process in MGPT-PU 104795 is broken, comparison with C3 vertebrae of extant porcupines suggests that the maximum measurable height is very close to the original measurement (only 0.5 mm were added). The more fragmentary specimen MGPT-PU 126233 (Figs.1b and 5pet) displays a similar overall morphology to MGPT-PU 104795, but it is assigned to C4 based on the slightly more ventrally-developed and less caudally-oriented transverse processes. This specimen similarly differs from extant Hystrix C4 (Fig. 5feo) in the more elliptical endplates, the better developed spinous process and the somewhat more ventral zygapophyses, but its overall morphology is completely porcupine-like. The lower cervical region is better represented among the Pirro Nord sample, with as many as four specimens attributable to level C5 (Fig. 1cef). The most complete ones include the previously unpublished specimens MGPT-PU 104796 (Figs. 1c and 6pet) and MGPT-PU 104797 (Fig. 1d). Their attribution to C5 is supported by the stouter and more transversely-aligned transverse processes, with well-developed ventral portions and costal processes, and the relatively wider overall proportions, together with the lack of the more distinctive features of C6. As in the preceding specimens, the Pirro Nord vertebrae are larger and stouter than those of extant Hystrix, with wider endplates and less dorsally-situated zygapophyses, further displaying more transversely-aligned transverse processes. Despite some damage in the dorsal-most portion of the spinous processes, these specimens were included in the morphometric analyses. Comparisons of MGPT-PU 104796 with extant C5 vertebrae indicate that the spinous process is only slightly abraded (so that the maximum preserved height can be readily employed as a reliable estimate). In MGPT-PU 104797, about the dorsal-most quarter of the spinous process is missing, so vertebral height was corrected by multiplying the height of the process of this specimen by a factor of 1.33. Unlike the two specimens mentioned above, MGPT-PU 126716 (Fig. 1e) is very

incomplete, lacking the upper-most portion of the neural arch and the whole spinous process, as well as part of the right prezygapophysis and a large portion of both transverse processes. However, a tentative assignment to C5 is also warranted for this specimen, based on the relatively well-developed and transversely-aligned transverse processes (which exclude an assignment to C3eC4) and the lack of the distinctive features of C6 (e.g., more tall than broad vertebral body) or C7 (e.g., very low situation of the pre- and postzygapophyses, smaller transverse foramina). Such an assignment is further supported by overall similarities with more complete specimens attributable to C5 (Fig. 1c,d and f), The specimens previously published by Rook et al. (2004) were previously assigned to C3 (PN34/1), C5 (PN34/2) and C6 (PN34/3). An unambiguous identification of cervical level for the more fragmentary specimen (PN34/1; Figs. 1f and 6uey), previously assigned to level C3, is difficult because the transverse processes are broken away. However, both overall proportions and the moderately well developed root of the transverse processes strongly suggest an attribution to level C5, as discussed above for the newly reported specimens MGPT-PU 104796, MGPT-PU 104797 and MGPT-PU 126716. Given the association between the three vertebrae originally reported by Rook et al. (2004), our cervical level assignment is in further agreement with the identification by these authors of the other somewhat fragmentary specimen to a C6 (PN34/3; Figs. 1g and 7pet). This assignment can be confidently confirmed by the very ventral situation of the pre- and postzygapophyses, the very transversely-oriented transverse processes with a large and protruding ventrocaudal extension, and the distinct and well developed ventral keel. In contrast, the identification of the most complete specimen PN34/2 (Figs.1h and 8pet) as a C5 by Rook et al. (2004) is at odds with the morphology of the transverse processes of this specimen (Fig. 7), which are very stout and completely transversely aligned (even somewhat cranially directed), and further lack entirely a ventrocaudal extension. The presence of caudal costal foveae cannot be ascertained because the caudal endplate is missing. However, the morphology of the transverse processes, coupled with the relatively tall vertebral foramen, the very low position of the pre- and postzygapophyses, the relatively small transverse foramina (compared with the other PN 34

specimens), the proportions of the vertebral body (wider than tall), and the tall spinous process, enable a secure assignment of this vertebra to level C7. Another previously-unpublished specimen (MGPT-PU 126234; Fig. 1i) is also assigned to C7, based on the restricted development of the transverse foramina and the very wide vertebral body, although its very fragmentary preservation precludes a completely secure assessment. Overall, like the other specimens from Pirro Nord first described here, the vertebrae described by Rook et al. (2004) closely resemble in morphology extant Hystrix cervical vertebrae, merely differing by being larger and stouter, as well as by displaying minor differences in the somewhat more ventral position of the zygapophyses, the wider vertebral bodies and endplates, and the more transversely-aligned transverse processes.

Morphometric comparisons

The general discriminant analysis (Table 2; Fig. 9), with cercopithecoid genera distinguished a priori and vertebral levels analyzed together, produced eight canonical discriminant functions (DF). A plot of the first two functions (Fig. 9a), which together explain 70.0% of the variance, distinguishes Hystrix from cercopithecids, with the former displaying much higher values of both DF1 (mainly resulting from tall vertebral bodies and narrow vertebral foramina) and DF2 (mostly attributable to low vertebral heights). The most complete vertebra from Pirro Nord among those previously reported by Rook et al. (2004), and here identified as a C7 (PN34/2), clearly departs from cercopithecid centroids in the same respects than extant Hystrix specimens do. PN34/2, in particular, shows a DF1 value beyond that of any cercopithecid and very similar to the Hystrix centroid, whereas in DF2 it only minimally overlaps with extreme cercopithecid values and also falls much closer to the Hystrix centroid. The three newly-reported specimens from Pirro Nord included in the analysis, including a C3 (MGPT-PU 104795) and two C5 (MGPT-PU 104797 and MGPT-PU 104796), also fall much closer to the Hystrix centroid than to those of any cercopithecoid. This discriminant analysis correctly classifies 56.7% of the original cases (43.8% when cross-validation is employed), showing that the vertebral measurements employed provide

poor discrimination at the genus level (as noted by Patel et al., 2007). Most of the misclassifications, however, occur among cercopithecids, since all of the porcupine vertebrae are correctly classified (although only 80% are correctly classified when using cross-validation, with the C7 of H. cristata and H. indica classified as Cercocebus and Mandrillus, respectively). Similarly, in only a single instance, a cercopithecid vertebra (a C5 of Macaca) is misclassified as porcupine. These results therefore suggest that, despite providing a poor discrimination among cercopithecid genera, our discriminant analysis performs remarkably well for distinguishing between monkeys and porcupines based on cervical vertebral measurements (Table 3). In fact, our analysis does not perform worse than that of Patel et al. (2007) for classifying Theropithecus vertebrae. These two analyses are not entirely comparable, not only because we included porcupines in the analysis, but also because Patel et al. (2007) analyzed vertebral levels separately (based on individual data), whereas we analyzed levels C3 to C5 together (based on sex-species mean values). The discriminant analysis by Patel et al. (2007, their Tables 4e7), in any case, correctly classified 56% (18/32) of included vertebrae of T. gelada, whereas that performed in this paper correctly classified 70% of the 10 sex-species means of Theropithecus for the various vertebral levels investigated (Table 3). It is thus most remarkable that the analyzed Pirro Nord vertebrae are in all instances much closer to the extant Hystrix centroid than to the closest cercopithecid centroid (Table 3), which corresponds to Papio (PN34/2, MGPT-PU 104796 and MGPT-PU 104797) or Theropithecus (MGPT-PU 104795). The analysis thus unambiguously classifies the Pirro Nord vertebrae as porcupine (Table 3), with a probability of group membership that is only statistically significant in two specimens (indicating that they differ from the morphology of extant Hystrix), but with a posterior probability of belonging to one of the a priori defined groups greater than 0.99 for Hystrix (Table 3). A cluster analysis based on the centroids of extant taxa (Fig. 9b) further shows that the Pirro Nord vertebrae cluster with extant Hystrix, well apart from the cercopithecids (all of which cluster together, with the similarities among taxa not reflecting the phylogeny of the group).

These results are confirmed by additional discriminant analyses performed for vertebral levels C3, C5 and C7 separately, but with all cercopithecoids grouped together (Table 4), which provide a highly satisfactory distinction between cercopithecoids and porcupines. Thus, for each analysis, 100% of the original cases are correctly classified, and when cross-validation is employed, the percentage of correctly-classified cases ranges from 98% (for the C5, in which a single specimen of Macaca sylvanus is misclassified as Hystrix) to 100% (for both C3 and C7). When the vertebrae from Pirro Nord are analyzed together with those from the extant comparative sample corresponding to the same cervical level, they are much closer to the porcupine than to the monkey centroid (Tables 4 and 5), being in all instances unambiguously classified as Hystrix. Body mass of the Pirro Nord porcupine Average tooth row lengths of 38.5 mm (upper) and 41.2 mm (lower) are computed for H. refossa from Pirro Nord based on the individual tooth measurements reported by Rook and Sardella (2013). Based on the allometric equations published by Freudenthal and Martín-Su_arez (2013) for hystricomorph rodents, these figures lead to a body mass estimate of about 25.7 kg (23.0 kg based on upper tooth row, and 28.5 kg based on lower tooth row). Discussion and conclusions When Rook et al. (2004) described the vertebrae from PN 34, only fused C3eC4 vertebrae of Theropithecus brumpti (KNM-WT 39368; Jablonski et al., 2002), too damaged to take reliable measurements (Patel et al., 2007), were available from the fossil record. More recently, Gilbert et al. (2011) reported a fairly complete cervical vertebra (likely somewhere between C3 and C6) of an adult female specimen of T. brumpti (KNM-TH 46700) from the Chemeron Formation. This specimen, however, has not been figured, and the brief description provided by Gilbert et al. (2011) merely suggests that the inclination of the apophyses (craniodorsal in the prezygapophyses, and caudoventral in the postzygapophyses) in T. brumpti was similar to that in T. gelada (and hence different from the Pirro Nord specimens). Although Rook et al. (2004) did not note the different inclination of the pre- and postzygapophyses in the Pirro Nord specimens compared with extant Theropithecus, they did recognize that the PN 34 vertebrae displayed some differences from extant geladas (i.e., more robust anterior tubercles of the costal processes as well as a stouter posterior

tubercles of the transverse processes). These differences were attributed by Rook et al. (2004) to the larger size of extinct Theropithecus species (e.g., 44 kg of average estimated body mass in T. oswaldi from Cueva Victoria; Delson et al., 2000) compared with extant geladas (average of 18 kg in males and 12 kg in females; Delson et al., 2000). Neither Rook et al. (2004) nor Patel et al. (2007) took into account that the Pirro Nord vertebrae might belong to a rodent (i.e., a 'micromammal') instead of any of the mammalian orders customarily considered 'macromammals' that are recorded at the site. At Pirro Nord, however, there are numerous specimens of the porcupine genus Hystrix (Rook and Sardella, 2005, 2013), which includes the largest species of extant OldWorld rodents (Sen,1999). Extant H. cristata has an average body mass of 11e12 kg (Mori and Lovari, 2014), and some populations of extant H. africaeaustralis are even larger (up to 17e18 kg of mean body mass; Barthelmess, 2006). The Pirro Nord porcupine was assigned by Rook and Sardella (2005, 2013; see also Salari and Sardella, 2011) to the Plio-Pleistocene species H. refossa (van Weers, 1994, 2005). This species is larger than both the Late Miocene Hystrix parvae (van Weers and Montoya, 1996) and the extant H. cristata, and more comparable in size to the Mio-Pliocene species Hystrix primigenia and Hystrix depereti (Sen, 2001; van Weers and Rook, 2003), although H. refossa displays even stouter and larger postcranial bones than the two latter species (Rook and Sardella, 2005). The morphological comparisons performed by us between extant Theropithecus and Hystrix cervical vertebrae indicate that the specimens from PN 34, together with previously-unpublished vertebrae from Pirro Nord with a similar morphology, show closer similarities with porcupines. Our comparisons further indicate that the cervical level assignment for the vertebrae described by Rook et al. (2004) is most likely C5eC6eC7, instead of C3eC6eC5 as originally reported. The morphological similarities of the Pirro Nord specimens with extant Hystrix are also confirmed by morphometric comparisons based on the metrical variables previously used by Patel et al. (2007). Although there are slight differences in size, robusticity and other minor morphological details (i.e., situation of zygapophyses and inclination of transverse processes) between the fossil specimens from Pirro Nord and the extant porcupine specimens studied by us

(Figs. 4e8; Table 1), they can be simply accounted for by the larger body size and stouter build of H. refossa compared with extant hystricids (Rook and Sardella, 2005). This is confirmed by the body mass estimate of about 26 kg for the Pirro Nord porcupine, computed here based on dental size. Although this estimate is very tentative, it suggests that H. refossa from Pirro Nord was significantly larger than extant H. cristata, as previously suggested based on the comparison of different anatomical elements (Rook and Sardella, 2005). This fact is in further agreement with the overall vertebral sizes of the Pirro Nord specimens (as measured by the geometric mean of vertebral measurements; Table 1), which are larger than those of H. cristata for all of the investigated vertebral levels. Given all of the evidence presented above, we formally attribute the cervical vertebrae from PN 34 and other vertebrae from Pirro Nord first reported here to the extinct porcupine H. refossa. It therefore follows that there is no longer any evidence for the record of Theropithecus at Pirro Nord. Thus, current evidence for the dispersal of Theropithecus out of Africa before ca. 1 Ma, when it is unambiguously recorded at Cueva Victoria (Gibert et al., 1995; Martínez-Navarro et al., 2005, 2008), exclusively consists of the calcaneus from ‘Ubeidiya, which has been somewhat tentatively assigned to the genus (Belmaker, 2010).

Acknowledgments

This work was funded by the Spanish Ministerio de Economía y Competitividad (CGL2011-28681, CGL2010-15326, and RYC-2009- 04533 to D.M.A.), the Generalitat de Catalunya (2009 SGR 754 GRC and 2009 SGR 324 GRC) and the Italian Ministero dell’Istruzione dell'Università e della Ricerca (PRIN 2012MY8AB2 to M.D.). Background work for this contribution has been possible thanks to the financial support by the Universit_a di Firenze (Fondi di Ateneo to L.R.) for a wider project on Neogene and Quaternary land mammal faunas.We thank Professor Giulio Pavia (coordinator) and all of the people who made possible the fieldwork at Pirro Nord led by the Università di Torino during 2004e2009. We also thank Eileen Westwig (AMNH) for access to extant comparative material, and the Associate Editor, two anonymous reviewers, and E. Delson for

helpful comments and suggestions on a previous version of this paper. We dedicate this work to the late Professor F. Clark Howell, who participated in the first study of the Pirro Nord cervical vertebrae and contributed most significantly to the development of paleontological studies on the European Early Pleistocene.

References

Arzarello, M., Marcolini, F., Pavia, G., Pavia, M., Petronio, C., Petrucci, M., Rook, L., Sardella, R., 2007. Evidence of earliest human occurrence in Europe: the site of Pirro Nord (Southern Italy). Naturwissenschaften 94, 107e112.

Arzarello, M., Marcolini, F., Pavia, G., Pavia, M., Petronio, C., Petrucci, M., Rook, L., Sardella, R., 2009. L'industrie lithique du site Pl_eistoc_ene inf_erieur de Pirro Nord (Apricena, Italie du sud): une occupation humaine entre 1,3 et 1,7 Ma. L'Anthropologie 113, 47e58.

Arzarello, M., Pavia, G., Peretto, C., Petronio, C., Sardella, R., 2012. Evidence of an Early Pleistocene hominin presence at Pirro Nord (Apricena, Foggia, southern Italy): P13 site. Quatern. Int. 267, 56e61.

Barthelmess, E.L., 2006. Hystrix africaeaustralis. Mamm. Spec. 788, 1e7.

Belmaker, M., 2010. The presence of a large cercopithecine (cf. Theropithecus sp.) in the ‘Ubeidiya formation (Early Pleistocene, Israel). J. Hum. Evol. 58, 79e89.

Delson, E., 1993. Theropithecus fossils from Africa and India and the taxonomy of the genus. In: Jablonski, N.G. (Ed.), Theropithecus: The Rise and Fall of a Primate Genus. Cambridge University Press, Cambridge, pp. 157e189.

Delson, E., Terranova, C.J., Jungers, W.L., Sargis, E.J., Jablonski, N.G., Dechow, P.C., 2000. Body mass in Cercopithecidae (Primates, Mammalia): estimation and scaling in extinct and extant taxa. Anthropol. Papers Am. Mus. Nat. Hist. 83, 1e159.

Freudenthal, M., Martín-Su_arez, E., 2013. Estimating body mass of fossil rodents. Scripta Geol. 145, 1e130.

Frost, S.R., Alemseged, Z., 2007. Middle Pleistocene fossil Cercopithecidae from Asbole, Afar Region, Ethiopia. J. Hum. Evol. 53, 227e259.

Gibert, J., Ribot, F., Gibert, L., Leakey, M., Arribas, A., Martinez, B., 1995. Presence of the cercopithecid genus Theropithecus in Cueva Victoria (Murcia, Spain). J. Hum. Evol. 28, 487e493.

Gibert, J., Gibert, L., Ribot, F., Ferr_andez-Canadell, C., S_anchez, F., Iglesias, A., Walker, M.J., 2008. CV-0, an early Pleistocene human phalanx from Cueva Victoria (Cartagena, Spain). J. Hum. Evol. 54, 150e156.

Gilbert, C.C., 2013. Cladistic analysis of extant and fossil African papionins using craniodental data. J. Hum. Evol. 64, 399e433.

Gilbert, C.C., Goble, E.D., Kingston, J.D., Hill, A., 2011. Partial skeleton of Theropithecus brumpti (Primates, Cercopithecidae) from the Chemeron Formation of the Tugen Hills, Kenya. J. Hum. Evol. 61, 347e362.

Gupta, V.J., Sahni, A., 1981. Theropithecus delsoni, a new cercopithecine species from the Upper Siwaliks of India. Bull. Geol. Soc. India 14, 69e71.

Hammer, Ø., Harper, D.A.T., 2006. Paleontological Data Analysis. Blackwell Publishing, Malden.

Hammer, Ø., Harper, D.A.T., Ryan, P.D., 2001. PAST: Paleontological statistics software package for education and data analysis. Palaeontol. Electr. 4. Art. 4.

Hughes, J.K., Elton, S., O'Regan, H.J., 2008. Theropithecus and 'Out of Africa' dispersal in the Plio-Pleistocene. J. Hum. Evol. 54, 43e77.

Jablonski, N.G., 2002. Fossil Old World monkeys: the late Neogene radiation. In: Hartwig, W.C. (Ed.), The Primate Fossil Record. Cambridge University Press, Cambridge, pp. 255e299.

Jablonski, N., Frost, S., 2010. Cercopithecoidea. In: Werdelin, L., Sanders, W.J. (Eds.), Cenozoic Mammals of Africa. University of California Press, San Diego, pp. 393e428.

Jablonski, N.G., Leakey, M.G., Kiarie, C., Ant_on, M., 2002. A new skeleton of Theropithecus brumpti (Primates: Cercopithecidae) from Lomekwi, West Turkana, Kenya. J. Hum. Evol. 43, 887e923.

Jungers, W.L., Falsetti, A.B., Wall, C.E., 1995. Shape, relative size, and sizeadjustments in morphometrics. Yearb. Phys. Anthropol. 38, 137e161.

Lopez, L., 2013. Atlas radiographique et ost_eologique du porc-_epic : Hyxtrix indica. Th_ese d'exercice. M_edicine v_et_erinaire, _Ecole Nationale V_et_erinaire de Toulouse.

Martínez-Navarro, B., Claret, A., Shabel, A.B., P_erez-Claros, J.A., Palmqvist, P., 2005. Early Pleistocene "hominid remains" from southern Spain and the taxonomic assignment of the Cueva Victoria phalanx. J. Hum. Evol. 48, 517e523.

Martínez-Navarro, B., Palmqvist, P., Shabel, A.B., P_erez-Claros, J.A., Lorenzo, C., Claret, A., 2008. Reply to Gibert et al. (2008) on the supposed human phalanx from Cueva Victoria (Cartagena, Spain). J. Hum. Evol. 54, 157e161.

Martínez-Navarro, B., Belmaker, M., Bar-Yosef, O., 2012. The bovid assemblage (Bovidae, Mammalia) from the Early Pleistocene site of 'Ubeidiya, Israel: Biochronological and paleoecological implications for the fossil and lithic bearing strata. Quatern. Int. 267, 78e97.

Milligan, G.W., 1980. An examination of the effect of six types of error perturbation on fifteen clustering algorithms. Psychometrika 45, 325e342.

Mori, E., Lovari, S., 2014. Sexual size monomorphism in the crested porcupine (Hystrix cristata). Mamm. Biol. 79, 157e160.

Mosimann, J.E., 1970. Size allometry: Size and shape variables with characterizations of the lognormal and generalized gamma distributions. J. Am. Stat. Assoc. 65, 930e945.

Patel, B.A., Gilbert, C.C., Ericson, K.E., 2007. Cercopithecoid cervical vertebral morphology and implications for the presence of Theropithecus in early Pleistocene Europe. J. Hum. Evol. 52, 113e129.

Pavia, M., Zunino, M., Coltorti, M., Angelone, C., Arzarello, M., Bagnus, C., Bellucci, L., Colombero, S., Marcolini, F., Peretto, C., Petronio, C., Petrucci, M., Pieruccini, P., Sardella, R., Tema, E., Villier, B., Pavia, G., 2012. Stratigraphical and palaeontological data from the Early Pleistocene Pirro 10 site of Pirro Nord (Puglia, south eastern Italy). Quatern. Int. 267, 40e55.

Pickford, M., 1993. Climatic change, biogeography, and Theropithecus. In: Jablonski, N.G. (Ed.), Theropithecus: The Rise and Fall of a Primate Genus. Cambridge University Press, Cambridge, pp. 227e243.

Roberts, P., Delson, E., Miracle, P., Ditchfield, P., Roberts, R.G., Jacobs, Z., Blinkhorn, J., Ciochon, R.L., Fleagle, J.G., Frost, S.R., Gilbert, C.C., Gunnell, G.F., Harrison, T., Korisettar, R., Petraglia, M.D., 2014. Continuity of mammalian fauna over the last 200,000 y in the Indian subcontinent. Proc. Natl. Acad. Sci. 111, 5848e5853.

Rook, L., 2009. The Italian fossil primate record: an update and perspectives for future research. Boll. Soc. Paleontol. It. 48, 67e77.

Rook, L., Martínez-Navarro, B., 2013. The large sized cercopithecoid from Pirro Nord and the importance of Theropithecus in the Early Pleistocene of Europe: faunal marker for hominins dispersal outside Africa. Palaeontogr. A 298, 107e112.

Rook, L., Sardella, R., 2005. Hystrix refossa Gervais, 1852 from Pirro Nord (Early Pleistocene, Southern Italy). Riv. It. Paleontol. Stratigr. 111, 489e496.

Rook, L., Sardella, R., 2013. New data on the Early Pleistocene large sized porcupine from Pirro Nord (Apricena, Apulia, Italy). Palaeontogr. A 298, 87e94.

Rook, L., Martínez-Navarro, B., Howell, F.C., 2004. Occurrence of Theropithecus sp. in the Late Villafranchian of southern Italy and implication for Early Pleistocene “out of Africa” dispersals. J. Hum. Evol. 47, 267e277.

Salari, L., Sardella, R., 2011. Il genere Hystrix Linnaeus, 1758 in Italia nel Pleistocene. Atti Soc. Tosc. Sci. Nat. Mem. A 116, 171e178.

Schultz, A.H., 1961. Lieferung 5: Vertebral column and thorax. In: Hofer, H., Schultz, A.H., Starck, D. (Eds.), Primatologia: Handbuch der Primatenkunde, IV. S. Karger, Basel.

Sen, S., 1999. Family Hystricidae. In: R€ossner, E., Heissig, K. (Eds.), The Miocene Land Mammals of Europe. Verlag Dr. Friedrich Pfeil, München, pp. 427e434.

Sen, S., 2001. Early Pliocene porcupine (Mammalia, Rodentia) from Perpignan, France: a new systematic study. Geodiversitas 23, 303e312.

van Weers, D.J., 1994. The porcupine Hystrix refossa Gervais, 1852 from the Plio- Pleistocene of Europe, with notes on other fossil and extant species of the genus Hystrix. Scripta Geol. 106, 35e52.

van Weers, D.J., 2005. A taxonomic revision of the Pleistocene Hystrix (Hystricidae, Rodentia) from Eurasia with notes on the evolution of the family. Contrib. Zool. 74, 301e312.

van Weers, D.J., Montoya, P., 1996. Taxonomy and stratigraphic record of the oldest European porcupine Hystrix parvae (Kretzoi, 1951). Proc. Kon. Ned. Akad. v. Wetensh. 99, 131e141.

van Weers, D.J., Rook, L., 2003. Turolian and Ruscinian porcupines (genus Hystrix, Rodentia) from Europe, Asia and North Africa. Pal€aontol. Z. 77, 95e113.

Ward, J.H., 1963. Hierarchical grouping to optimize an objective function. J. Am. Stat. Assoc. 58, 236e244.

Yilmaz, S., 1998. Macro-anatomical investigations on the skeletons of porcupine (Hystrix cristata). Part III: Skeleton axiale. Anat. Histol. Embryol. 27, 293e296.

Tables and Figures Captions

Table 1

Cervical vertebral measurementsa (in mm) for extant Hystrix spp. as well as the Pirro Nord specimens.

Taxon Level GBtp Bpa H Bf Hf Bfcr Hfcr Lvb GM

H. cristata (mean, N ¼ 3)b C3 32.27 23.97 24.93 11.47 9.27 13.00 10.10 12.80 15.54

H. indica (N ¼ 1)b C3 26.40 23.90 23.00 10.50 9.00 13.30 10.10 12.20 14.76

Pirro Nord (MGPT-PU 104795)c C3 34.60 26.20 (31.00)g 13.30 10.90 16.60 14.30 10.80 (17.88)

H. cristata (mean, N ¼ 3)b C4 33.77 28.10 25.67 11.50 9.20 12.70 11.30 12.67 16.13

H. indica (N ¼ 1)b C4 29.40 26.10 22.80 11.10 8.60 13.20 10.40 11.80 15.10

Pirro Nord (MGPT-PU 126233)c C4 e >26.60 e 12.50 11.50 16.10 (9.80) 11.60 e

H. cristata (mean, N ¼ 3)b C5 33.83 28.27 26.57 12.13 9.83 12.77 11.50 12.20 16.46

H. indica (N ¼ 1)b C5 30.90 26.40 26.00 11.10 9.50 13.00 10.80 11.40 15.64

Pirro Nord (PN34/1)d C5e e 32.10 e 14.90 12.50 15.00 10.45 13.88h e

Pirro Nord (MGPT-PU 104796)c C5 41.40 34.00 (31.80) 13.90 11.70 15.40 10.30 (13.30)h (18.76)

Pirro Nord (MGPT-PU 104797)c C5 (43.00) 33.70 (30.10)g 13.50 10.70 17.40 10.80 12.70 (18.71)

Pirro Nord (MGPT-PU 126716)c C5 (41.20) (25.00) e 12.20 e (17.80) (12.10) >9.20 e

H. cristata (mean, N ¼ 3)b C6 35.17 27.83 28.77 12.10 11.27 12.23 12.27 12.63 17.07

H. indica (N ¼ 1)b C6 33.20 27.00 28.70 11.20 9.90 12.50 11.20 12.20 16.25

Pirro Nord (PN34/3)d C6 45.20 35.45 (31.80) 14.50 12.30 (17.20) (14.20) >11.30 e

H. cristata (mean, N ¼ 3)b C7 35.17 27.83 28.77 12.10 11.27 12.23 12.27 12.63 17.07

H. indica (N ¼ 1)b C7 36.20 27.90 38.90 11.50 11.20 12.10 13.30 11.60 17.66

Pirro Nord (PN34/2)d C7f 43.90 33.00 37.50 14.05 13.15 16.70 13.00 13.88h 20.42

Pirro Nord (MGPT-PU 126234)c C7 e >29.60 e 14.80 12.60 (16.60) (10.10) >8.50 e

Abbreviations: GBtp, Greatest breadth across the posterior tubercle; Bpa, Greatest breadth across the prezygapophyses; H, greatest height; Bf, maximum breadth of vertebral foramen; Hf, maximum height of vertebral foramen; Bfcr, breadth of the vertebral body cranial articular surface; Hfcr, height of the vertebral body cranial articular surface; Lvb, ventral length of the vertebral body; GM, geometric mean.

a Measurements after Rook et al. (2004) and Patel et al. (2007, their Fig. 2).

b Specimens measured by D.M.A. Catalog numbers: H. cristata (AMNH 87220, AMNH 119506 and AMNH 216336); H. indica (AMNH 14144).

c New specimens reported in this study. Values between parentheses are estimates.

d Data taken from Rook et al. (2004), except for H in the C6 specimen, which can be estimated based on the maximum preserved measurements.

e Identified by Rook et al. (2004) as a C3.

f Identified by Rook et al. (2004) as a C5.

g H corrected by adding 0.5 mm in MGPT-PU 104795 and by multiplying the height of the spinous process by 1.33 in MGPT-PU 104797 (maximum preserved height
28.1 mm).

h Lvb corrected by dividing the original measurement by 0.9 (to account for the lack of the caudal endplate).

Table 2

Results of the discriminant analysis (see also Fig. 9) based on Mosimann shape variables of cervical vertebrae C3eC7 in a sample of extant cercopithecid primates (grouped by
genus) and porcupines, as well as discriminant scores for selected taxa (Theropithecus, Hystrix and the Pirro Nord most complete vertebrae). The classifications for the Pirro
Nord vertebrae are reported in Table 3.

	DF1	DF2	DF3	DF4	DF5	DF6	DF7	DF8
Canonical discriminant functions								
Eigenvalue	2.355	1.574	0.839	0.366	0.246	0.155	0.058	0.021
% variance	42.0	28.0	14.9	6.5	4.4	2.8	1.0	0.4
Cumulative % variance	42.0	70.0	84.9	91.5	95.8	98.6	99.6	100.0

Canonical correlation 0.838 0.782 0.675 0.518 0.444 0.366 0.234 0.142

Standardized canonical discriminant function coefficients

GBtp/GM _0.476 0.403 1.095 _0.470 0.698 0.036 _0.095 0.618

Bpa/GM 0.117 0.057 _0.041 0.075 0.025 0.920 _0.548 0.480

H/GM 0.404 _0.917 0.267 0.307 _0.268 0.092 0.059 0.412

Bf/GM _0.432 _0.226 _0.529 0.988 _0.374 _0.404 0.058 0.609

Hf/GM _0.102 0.067 0.416 _1.058 0.627 0.413 0.618 0.468

Bfcr/GM 0.329 0.014 0.137 _0.525 _0.572 _0.057 _0.466 0.610

Hfcr/GM 0.573 0.327 _0.133 0.321 0.593 _0.064 0.208 0.421

Lvb/GM _0.112 0.296 0.796 0.516 _0.445 0.474 0.239 0.996

Structure matrix

Hfcr/GM 0.715 0.324 _0.123 0.221 0.434 _0.243 0.068 0.261

Bf/GM _0.570 _0.196 _0.522 0.048 0.105 _0.231 _0.003 0.545

H/GM 0.279 _0.859 0.351 0.143 0.187 _0.038 _0.052 0.046

Bfcr/GM 0.302 0.183 _0.138 _0.473 _0.406 _0.422 _0.321 0.431

Lvb/GM 0.105 0.438 0.368 0.244 _0.523 0.279 0.500 _0.022

Bpa/GM _0.157 _0.115 _0.311 0.074 0.267 0.704 _0.523 0.137

Hf/GM _0.213 _0.162 _0.397 _0.467 0.034 0.251 0.616 0.331

Gbtp/GM _0.296 _0.131 0.449 0.078 0.486 _0.351 _0.558 0.125

Functions at group centroids

Allenopithecus _1.441 0.430 0.798 1.230 0.677 _0.153 0.137 0.162

Cercocebus 0.067 0.092 _0.644 0.152 _0.394 _0.786 0.425 _0.156

Cercopithecus _1.996 0.944 1.138 _0.089 0.082 _0.042 _0.065 _0.247

Chlorocebus _2.132 0.432 0.147 _0.080 _0.380 _0.152 0.024 0.067

Colobus _0.317 _0.225 0.037 0.293 _0.859 _0.282 _0.252 0.161

Erythrocebus _0.048 0.329 2.342 1.239 0.379 0.627 0.657 0.257

Lophocebus _1.035 _1.118 0.719 _1.041 _1.025 _0.632 0.407 0.317

Macaca 0.183 _0.495 _0.566 _0.322 0.321 _0.222 0.142 _0.029

Mandrillus 1.743 _2.479 0.606 _0.083 0.115 0.675 0.230 _0.051

Nasalis 1.733 _0.585 _1.993 1.407 _0.995 0.173 0.061 _0.334

Papio 0.908 _1.161 0.787 _0.228 _0.054 0.144 _0.355 _0.005

Presbytis _0.513 0.384 _0.836 _0.348 _1.366 1.135 0.323 _0.135

Semnopithecus 0.455 _0.417 _0.412 2.447 0.127 _0.414 _0.136 0.000

Theropithecus 0.722 _0.153 _0.527 0.066 0.809 _0.252 _0.261 0.082

Trachypithecus _1.177 1.149 _1.174 _0.121 0.199 0.536 _0.100 0.117

Hystrix 4.416 3.623 0.650 _0.299 _0.168 _0.121 0.044 0.017

Discriminant scores for selected taxa

Theropithecus gelada \ C3 _0.009 _0.032 0.725 0.352 _0.558 _0.385 1.898 _0.061

Theropithecus gelada \ C4 _0.098 _0.376 _0.115 0.484 0.066 0.610 0.477 _0.228

Theropithecus gelada \ C5 0.319 _0.370 _0.414 _0.017 1.195 0.230 _0.136 _0.376

Theropithecus gelada \ C6 0.031 0.042 _0.164 _0.048 2.026 _0.614 _0.365 _0.188

Theropithecus gelada \ C7 1.288 0.815 _0.903 _0.041 1.183 _2.680 _2.056 0.600

Theropithecus gelada _ C3 1.262 _0.424 _0.276 0.013 0.329 _0.573 1.987 _0.326

Theropithecus gelada _ C4 1.341 0.230 _0.751 _0.137 0.785 1.003 _0.586 _0.302

Theropithecus gelada _ C5 1.315 _0.543 _0.772 _0.067 0.697 1.206 _0.946 0.665

Theropithecus gelada _ C6 0.923 _0.708 _1.323 0.062 1.485 0.018 _1.141 0.676

Theropithecus gelada _ C7 0.845 _0.167 _1.280 0.061 0.877 _1.331 _1.746 0.362

Hystrix cristata C3 3.535 4.072 1.556 _0.378 _1.256 _0.537 0.049 0.999

Hystrix cristata C4 4.212 4.535 0.928 0.244 0.090 0.620 _0.553 0.829

Hystrix cristata C5 4.137 4.060 0.343 0.101 0.373 0.231 _0.226 0.416

Hystrix cristata C6 4.275 3.748 0.891 _0.401 1.711 0.187 1.229 0.040

Hystrix cristata C7 2.431 4.339 _0.705 _0.945 _1.165 _2.365 0.322 _5.182

Hystrix indica C3 4.907 4.350 0.524 _0.780 _1.905 0.067 _0.451 1.310

Hystrix indica C4 4.422 4.771 0.144 _0.269 _1.226 0.222 _1.218 1.056

Hystrix indica C5 4.797 3.553 0.387 _0.782 _0.312 0.133 _0.496 0.451

Hystrix indica C6 4.716 2.980 1.151 _0.273 0.220 0.343 0.192 0.325

Hystrix indica C7 6.724 _0.174 1.282 0.494 1.792 _0.114 1.592 _0.076

PN34/2 (C7) 4.625 1.707 1.093 _2.488 0.310 _0.322 _0.397 _0.205

MGPT-PU 104795 (C3) 6.746 3.051 _1.121 _1.167 0.338 _2.562 _0.121 0.474

MGPT-PU 104796 (C5) 2.638 2.601 1.471 _1.870 _1.291 1.077 _1.533 0.338

MGPT-PU 104797 (C5) 3.339 3.522 1.400 _2.761 _1.726 0.437 _2.841 0.738

Abbreviations: See Table 1.

Sex-species means for extant cercopithecoids taken from Patel et al. (2007, their Appendix; see their Table 1 for sample sizes).

Table 3

Classification results of the discriminant analysis (Table 2; Fig. 9) based on Mosimann shape variables of cervical vertebrae C3eC7 for Theropithecus, Hystrix and the Pirro Nord vertebrae.

1st PG p P D2 2nd PG P D2

Theropithecus gelada \ C3 Cercocebus 0.829 0.305 4.302 Colobus 0.178 5.383

Theropithecus gelada \ C4 Macaca 0.985 0.227 1.855 Colobus 0.167 2.466

Theropithecus gelada \ C5 Theropithecus 0.999 0.410 0.835 Macaca 0.323 1.316

Theropithecus gelada \ C6 Theropithecus 0.968 0.540 2.358 Macaca 0.250 3.894

Theropithecus gelada \ C7 Theropithecus 0.205 0.753 10.938 Cercocebus 0.103 14.919

Theropithecus gelada _ C3 Cercocebus 0.770 0.327 4.886 Macaca 0.312 4.983

Theropithecus gelada _ C4 Theropithecus 0.964 0.535 2.448 Macaca 0.217 4.253

Theropithecus gelada _ C5 Theropithecus 0.897 0.471 3.527 Macaca 0.201 5.236

Theropithecus gelada _ C6 Theropithecus 0.955 0.663 2.638 Macaca 0.217 4.871

Theropithecus gelada _ C7 Theropithecus 0.854 0.622 4.033 Macaca 0.185 6.460

Hystrix cristata C3 Hystrix 0.846 1.000 4.124 Erythrocebus 0.000 35.032

Hystrix cristata C4 Hystrix 0.942 1.000 2.878 Theropithecus 0.000 38.232

Hystrix cristata C5 Hystrix 0.997 1.000 1.171 Theropithecus 0.000 30.703

Hystrix cristata C6 Hystrix 0.743 1.000 5.134 Theropithecus 0.000 33.303

Hystrix cristata C7 Hystrix 0.000 0.999 39.838 Cercocebus 0.001 53.194

Hystrix indica C3 Hystrix 0.649 1.000 5.985 Theropithecus 0.000 48.616

Hystrix indica C4 Hystrix 0.705 1.000 5.486 Theropithecus 0.000 44.738

Hystrix indica C5 Hystrix 0.998 1.000 1.018 Theropithecus 0.000 33.492

Hystrix indica C6 Hystrix 0.996 1.000 1.238 Theropithecus 0.000 29.661

Hystrix indica C7 Hystrix 0.001 0.989 27.022 Mandrillus 0.010 36.195

PN34/2 (C7) Hystrix 0.324 1.000 9.216 Papio 0.000 27.632

MGPT-PU 104795 (C3) Hystrix 0.041 1.000 16.096 Theropithecus 0.000 54.168

MGPT-PU 104796 (C5) Hystrix 0.125 0.994 12.637 Papio 0.003 24.215

MGPT-PU 104797 (C5) Hystrix 0.013 1.000 19.376 Papio 0.000 44.239

Abbreviations: PG, predicted group; p, classification probability (i.e., probability of group membership given a particular discriminant score); P, posterior probability of group membership (i.e., probability of belonging to one of the groups defined a priori, given equal prior probabilities for them); D2, squared Mahalanobis distance.

Table 4

Results of the three discriminant analyses (a single discriminant function each)

based on Mosimann shape variables of cervical vertebrae C3, C5 and C7 separately in

a sample of extant cercopithecid primates (all grouped together) and porcupines, as well as discriminant scores for selected taxa (Theropithecus, Hystrix and the Pirro Nord most complete vertebra). The classifications for the Pirro Nord vertebrae are reported in Table 5.

C3 C5 C7

Canonical discriminant function

Eigenvalue 5.810 3.535 4.193

% variance 100 100 100

Canonical correlation 0.924 0.883 0.899

Standardized canonical discriminant function coefficients

GBtp/GM 2.932 0.883 0.244

Bpa/GM 1.807 0.253 0.456

H/GM 2.528 0.115 0.497

Bf/GM 2.363 _0.092 0.771

Hf/GM 3.613 1.488 _0.582

Bfcr/GM 3.608 1.133 0.329

Hfcr/GM 4.400 1.563 _0.817

Lvb/GM 5.011 1.368 _0.295

Structure matrix

Hfcr/GM 0.297 0.415 _0.335

Bf/GM _0.304 _0.367 0.570

H/GM _0.170 _0.163 0.077

Bfcr/GM 0.308 0.421 _0.035

Lvb/GM 0.209 0.334 _0.334

Bpa/GM _0.081 _0.283 0.315

Hf/GM _0.214 _0.237 0.148

Gbtp/GM _0.135 _0.197 0.423

Function at group centroids

Cercopithecoidea _0.526 _0.405 0.470

Hystrix 10.520 8.312 _8.456

Discriminant scores for selected taxa

Theropithecus gelada \ _1.796 _0.757 0.491

Theropithecus gelada _ _0.917 1.088 0.858

Hystrix cristata C3 9.269 7.921 _8.213

Hystrix indica C3 11.771 8.704 _8.699

PN34/2 (C7) e e _6.342

MGPT-PU 104795 (C3) 12.334 e e

MGPT-PU 104796 (C5) e 6.119 e

MGPT-PU 104797 (C5) e 8.164 e

Abbreviations: See Table 1.

Sex-species means for extant cercopithecoids taken from Patel et al. (2007, their Appendix; see their Table 1 for sample sizes).

Table 5

Classification results of the three discriminant analyses (Table 4) based on Mosimann shape variables of cervical vertebrae C3, C5 and C7 separately for Theropithecus, Hystrix and the Pirro Nord vertebrae.

1st PG p P D2 2nd PG P D2

Discriminant analysis for C3

Theropithecus gelada \ Cercopithecoid 0.204 1.000 1.614 Hystrix 0.000 151.691

Theropithecus gelada _ Cercopithecoid 0.696 1.000 0.153 Hystrix 0.000 130.795

Hystrix cristata Hystrix 0.211 1.000 1.566 Cercopithecoid 0.000 95.934

Hystrix indica Hystrix 0.211 1.000 1.566 Cercopithecoid 0.000 151.219

MGPT-PU 104795 (C3) Hystrix 0.070 1.000 3.291 Cercopithecoid 0.000 165.382

Discriminant analysis for C5

Theropithecus gelada \ Cercopithecoid 0.726 1.000 0.123 Hystrix 0.000 82.247

Theropithecus gelada _ Cercopithecoid 0.135 1.000 2.229 Hystrix 0.000 52.198

Hystrix cristata Hystrix 0.696 1.000 0.153 Cercopithecoid 0.000 69.337

Hystrix indica Hystrix 0.696 1.000 0.153 Cercopithecoid 0.000 82.975

MGPT-PU 104796 (C5) Hystrix 0.028 1.000 4.811 Cercopithecoid 0.000 42.571

MGPT-PU 104797 (C5) Hystrix 0.882 1.000 0.022 Cercopithecoid 0.000 73.434

Discriminant analysis for C7

Theropithecus gelada \ Cercopithecoid 0.983 1.000 0.000 Hystrix 0.000 5.383

Theropithecus gelada _ Cercopithecoid 0.698 1.000 0.151 Hystrix 0.000 86.747

Hystrix cristata Hystrix 0.808 1.000 0.059 Cercopithecoid 0.000 75.389

Hystrix indica Hystrix 0.808 1.000 0.059 Cercopithecoid 0.000 84.062

PN34/2 (C7) Hystrix 0.035 1.000 4.467 Cercopithecoid 0.000 46.404

Abbreviations as in Table 3.

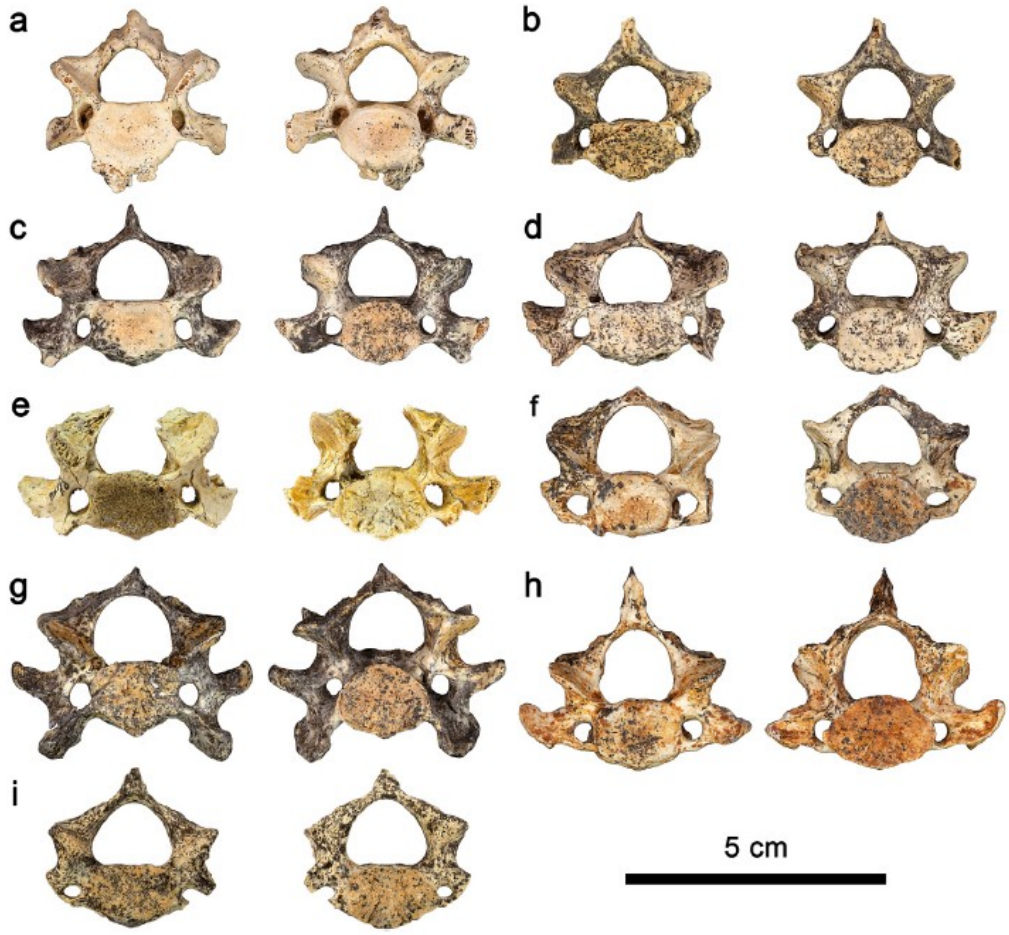

Figure 1. Cervical vertebrae from Pirro Nord previously attributed by Rook et al. (2004) to Theropithecus sp. (feh), compared with previously unpublished cervical vertebrae from the same locality (aee, i). All specimens are attributed here to Hystrix refossa, with estimated cervical level within parenthesis. a: MGPT-PU 104795 (C3); b: MGPT-PU 126233 (C4); c: MGPT-PU 104796 (C5); d: MGPT-PU 104797 (C5); e: MGPT-PU 126716 (C5); feh: Associated vertebrae PN34/1 (C5) e PN34/3 (C6) e PN34/2 (C7) from PN 34; i: MGPT-PU 126234 (C7). Each specimen is depicted in cranial (left) and caudal (right) views.

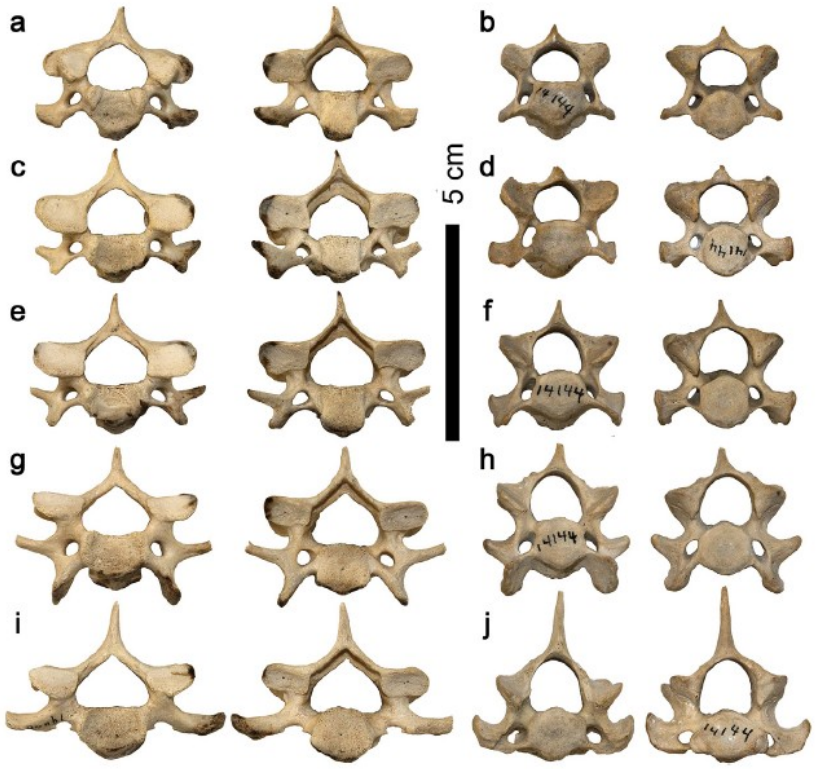

Figure 2. Cervical vertebrae C3eC7 of extant Theropithecus gelada (AMNH 19006; a, c, e, g, i) and Hystrix indica (AMNH 14144; b, d, f, h, j), showing the variation in morphology along the spine. For each taxon and vertebral level, both the cranial and caudal views are depicted (left and right, respectively). a, b: C3; c, d. C4; e, f: C5; g, h: C6; i, j: C7.

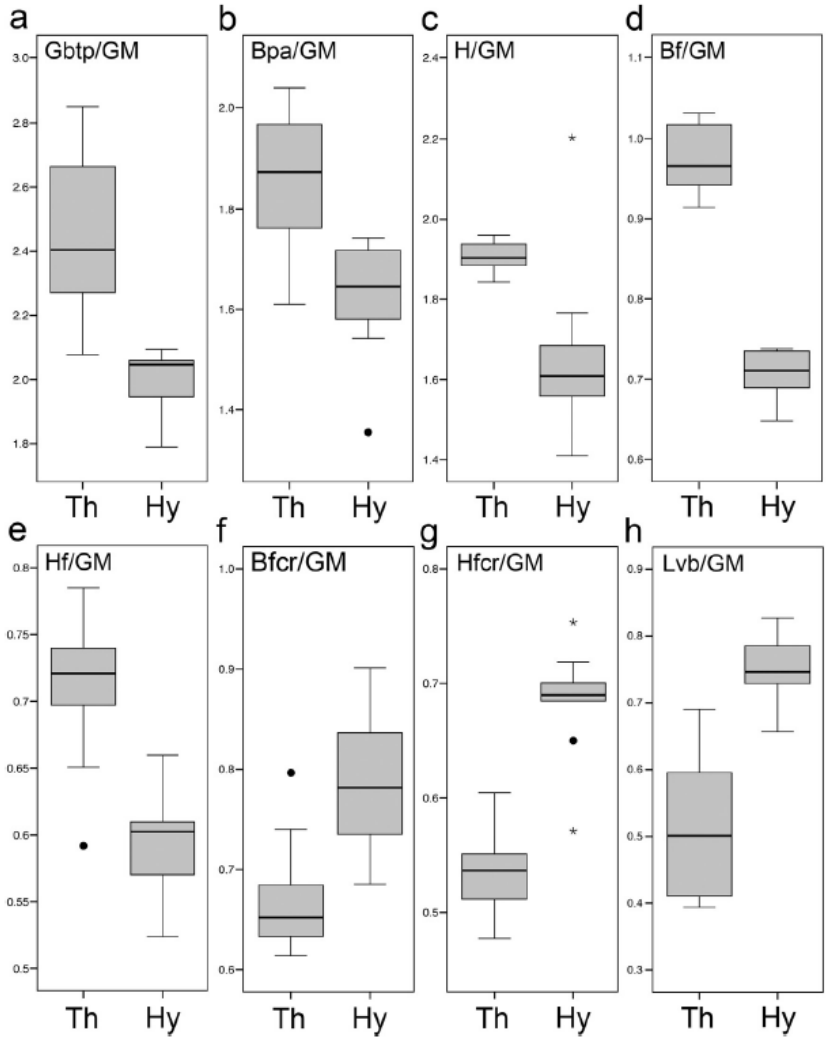

Figure 3. Boxplots depicting the Mosimann shape variables employed in the discriminant analyses in Theropithecus gelada and Hystrix spp., based respectively on sex-species and species mean values for vertebral levels C3 to C7. a, GBtp/GM; b, Bpa/GM; c, H/GM; d, Bf/GM; e, Hf/GM; f, Bfcr/GM; g, Hfcr/GM; h, Lvb/GM. Abbreviations: Th, T. gelada; Hy, Hystrix spp.; see Table 1 for variable abbreviations. Data for T. gelada taken from Patel et al. (2007, their Appendix). Box represents 25th and 75th percentiles, centerline is median, whiskers are nonoutlier range, dots are outliers, and stars represent extreme outliers. ANOVA comparisons indicate significant differences in all instances at $p < 0.001$ (Gbtp/GM, Bf/GM, Hf/ GM, Bfcr/GM, Hfcr/GM and Lvb/GM) or $p < 0.01$ (Bpa/GM and H/GM).

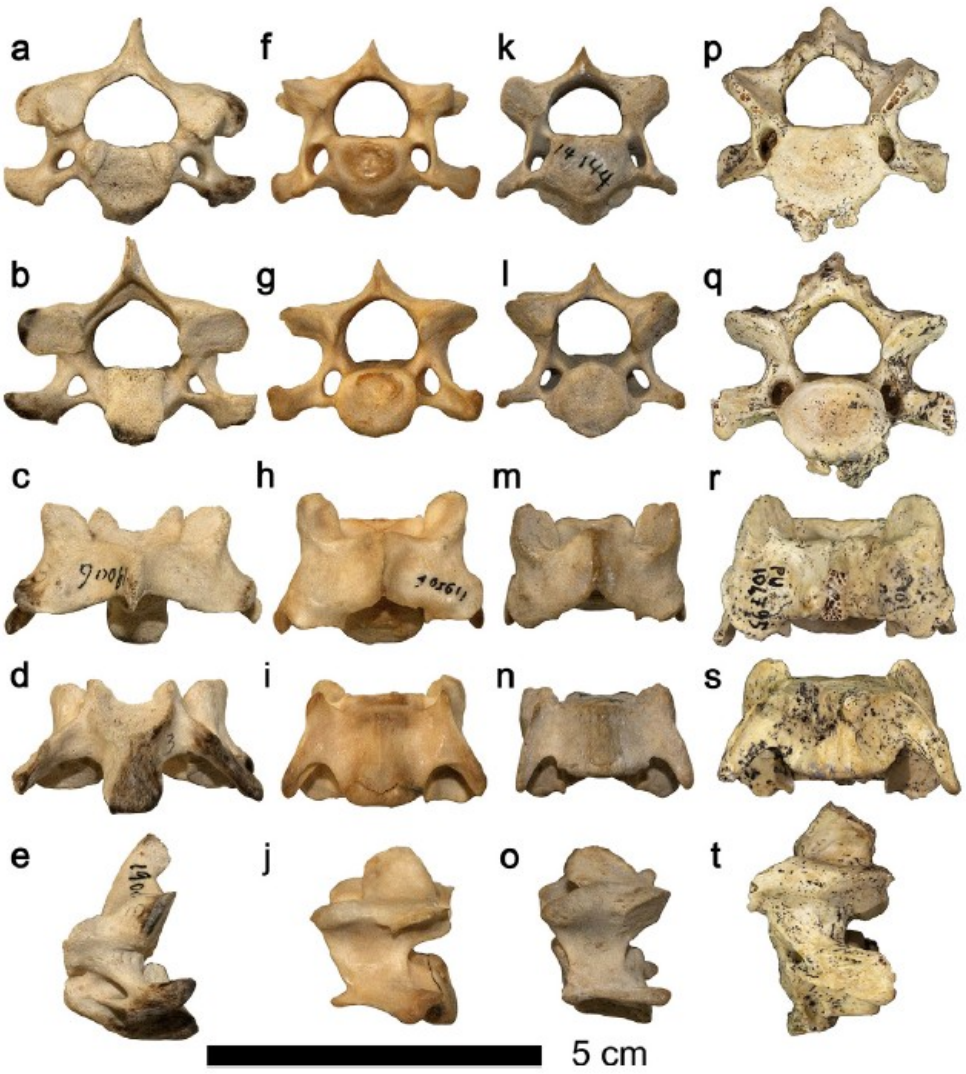

Figure 4. Cervical vertebra C3 in geladas, porcupines and Pirro Nord. aee: Theropithecus gelada (AMNH 19006), in cranial (a), caudal (b), dorsal (c), ventral (d) and left lateral (e) views; fej: Hystrix cristata (AMNH 119506), in cranial (f), caudal (g), dorsal (h), ventral (i) and left lateral (j) views; keo: Hystrix indica (AMNH 14144), in cranial (k), caudal (l), dorsal (m), ventral (n) and left lateral (o) views; pet: Hystrix refossa from Pirro Nord (MGPT-PU 104795), in cranial (p), caudal (q), dorsal (r), ventral (s) and left lateral (t) views.

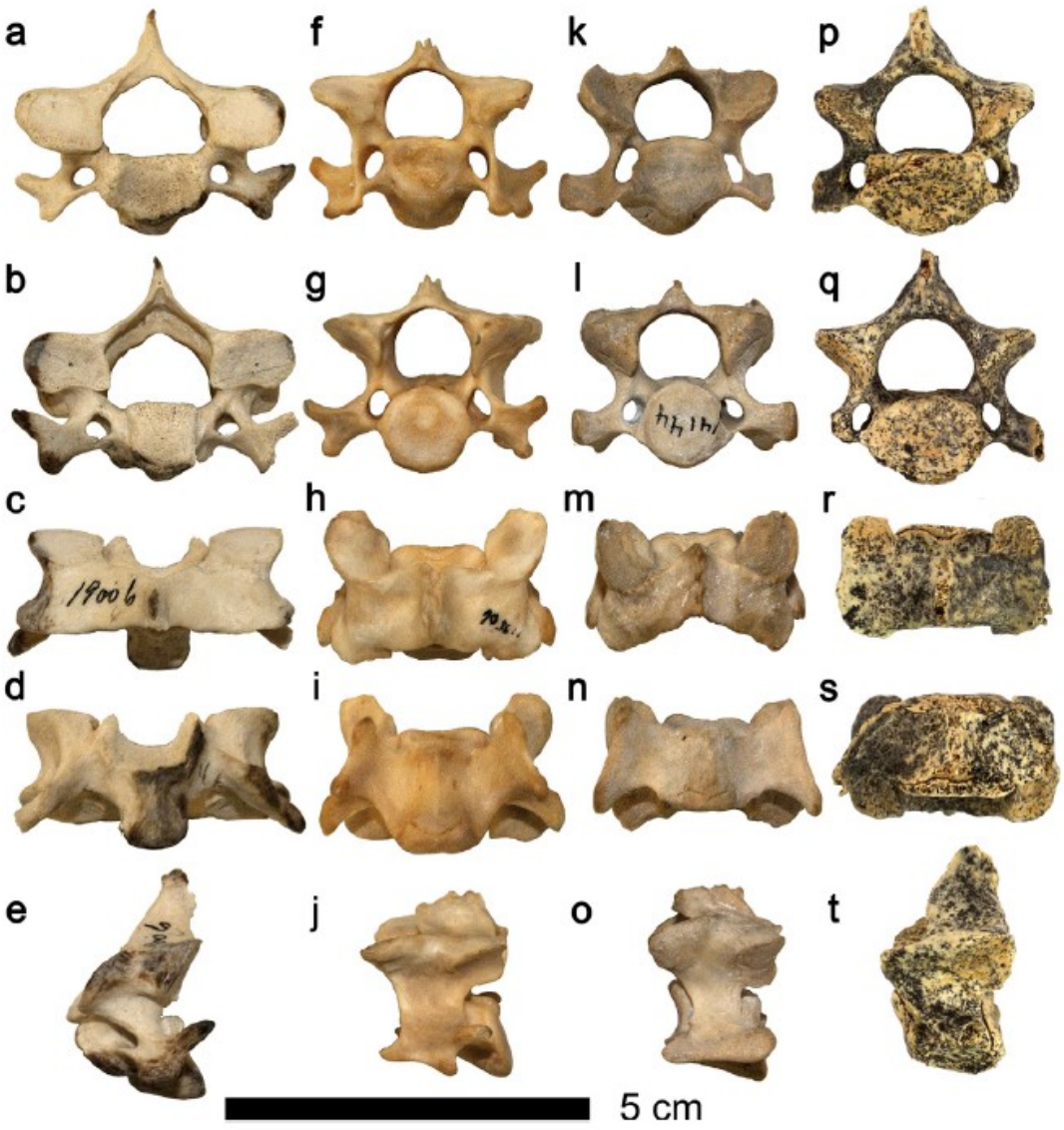

Figure 5. Cervical vertebra C4 in geladas, porcupines and Pirro Nord. aee: Theropithecus gelada (AMNH 19006), in cranial (a), caudal (b), dorsal (c), ventral (d) and left lateral (e) views; fej: Hystrix cristata (AMNH 119506), in cranial (f), caudal (g), dorsal (h), ventral (i) and left lateral (j) views; keo: Hystrix indica (AMNH 14144), in cranial (k), caudal (l), dorsal (m), ventral (n) and left

lateral (o) views; pet: Hystrix refossa from Pirro Nord (MGPT-PU 126233), in cranial (p), caudal (q), dorsal (r), ventral (s) and left lateral (t) views.

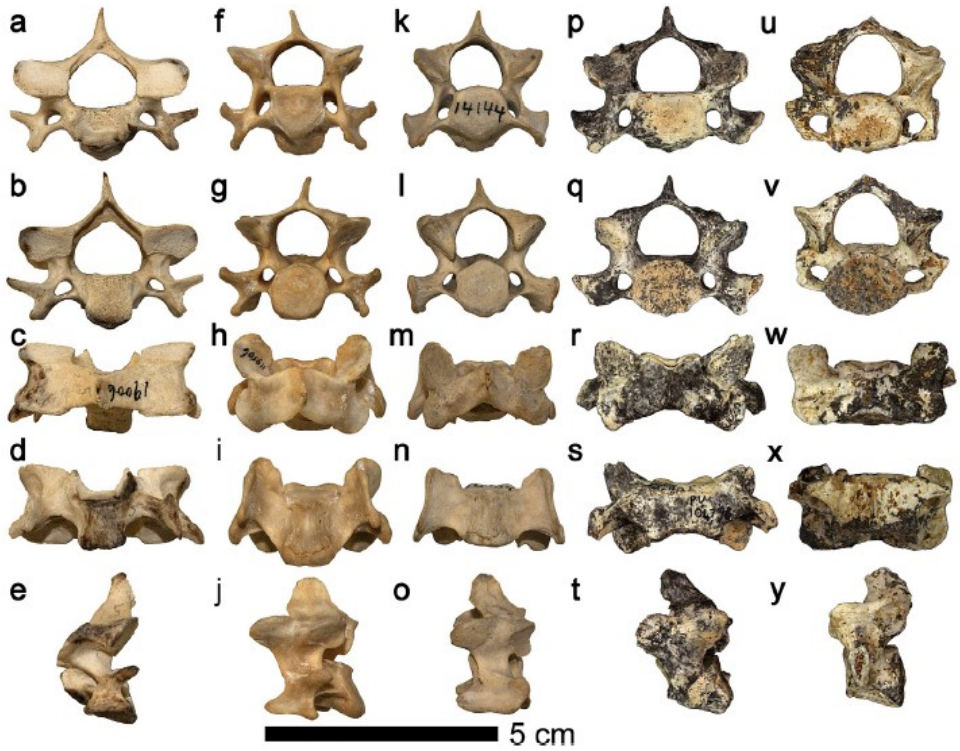

Figure 6. Cervical vertebra C5 in geladas, porcupines and Pirro Nord. aee: Theropithecus gelada (AMNH 19006), in cranial (a), caudal (b), dorsal (c), ventral (d) and left lateral (e) views; fej: Hystrix cristata (AMNH 119506), in cranial (f), caudal (g), dorsal (h), ventral (i) and left lateral (j) views; keo: Hystrix indica (AMNH 14144), in cranial (k), caudal (l), dorsal (m), ventral (n) and left lateral (o) views; pet: Hystrix refossa from Pirro Nord (MGPT-PU 104796), in cranial (p), caudal (q), dorsal (r), ventral (s) and left lateral (t) views; uey: H. refossa from Pirro Nord (PN34/1), in cranial (u), caudal (v), dorsal (w), ventral (x) and left lateral (y) views.

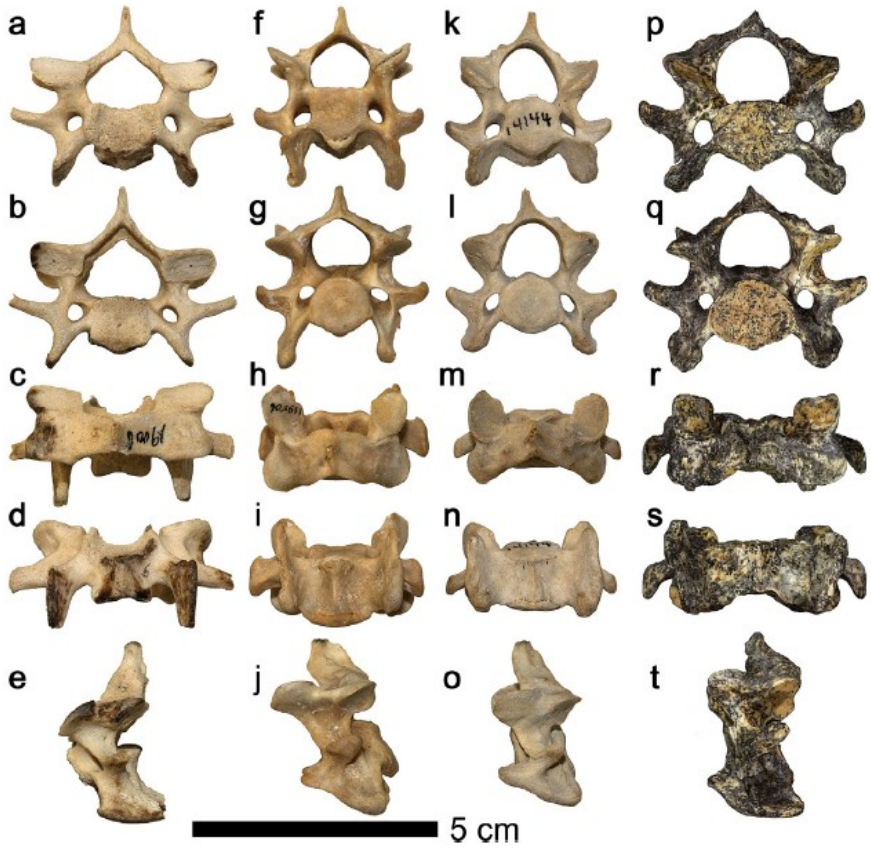

Figure 7. Cervical vertebra C6 in geladas, porcupines and Pirro Nord. aee. Theropithecus gelada (AMNH 19006), in cranial (a), caudal (b), dorsal (c), ventral (d) and left lateral (e) views; fej. Hystrix cristata (AMNH 119506), in cranial (f), caudal (g), dorsal (h), ventral (i) and left lateral (j) views; keo. Hystrix indica (AMNH 14144), in cranial (k), caudal (l), dorsal (m), ventral (n) and left lateral (o) views; pet. Hystrix refossa from Pirro Nord (PN34/3), in cranial (p), caudal (q), dorsal (r), ventral (s) and left lateral (t) views.

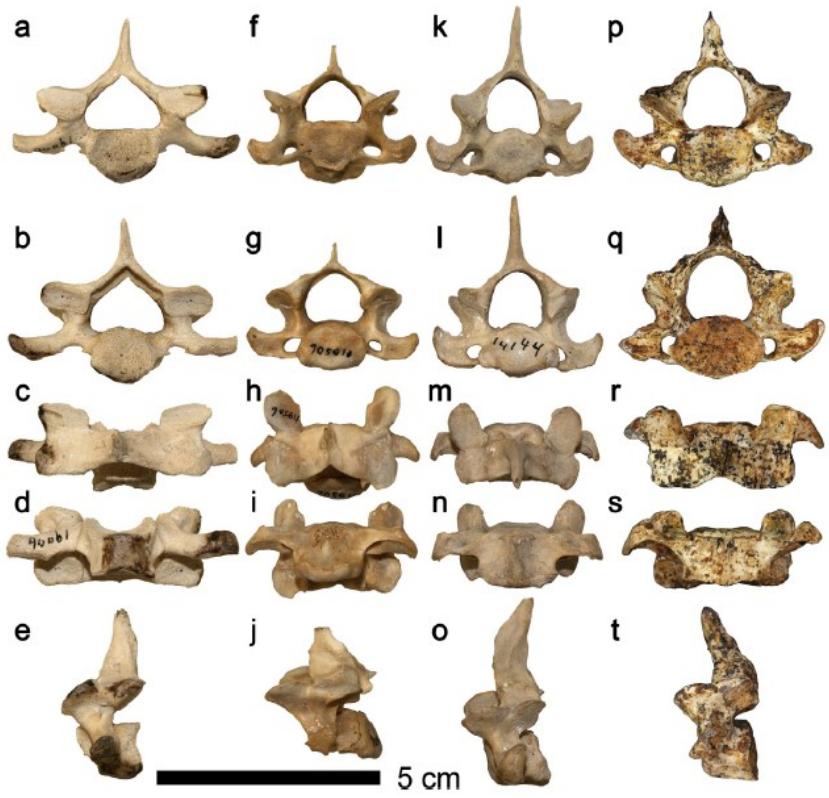

Figure 8. Cervical vertebra C7 in geladas, porcupines and Pirro Nord. aee. Theropithecus gelada (AMNH 19006), in cranial (a), caudal (b), dorsal (c), ventral (d) and left lateral (e) views; fej. Hystrix cristata (AMNH 119506), in cranial (f), caudal (g), dorsal (h), ventral (i) and left lateral (j) views; keo. Hystrix indica (AMNH 14144), in cranial (k), caudal (l), dorsal (m), ventral (n) and left lateral (o) views; pet. Hystrix refossa from Pirro Nord (PN34/2), in cranial (p), caudal (q), dorsal (r), ventral (s) and left lateral (t) views.

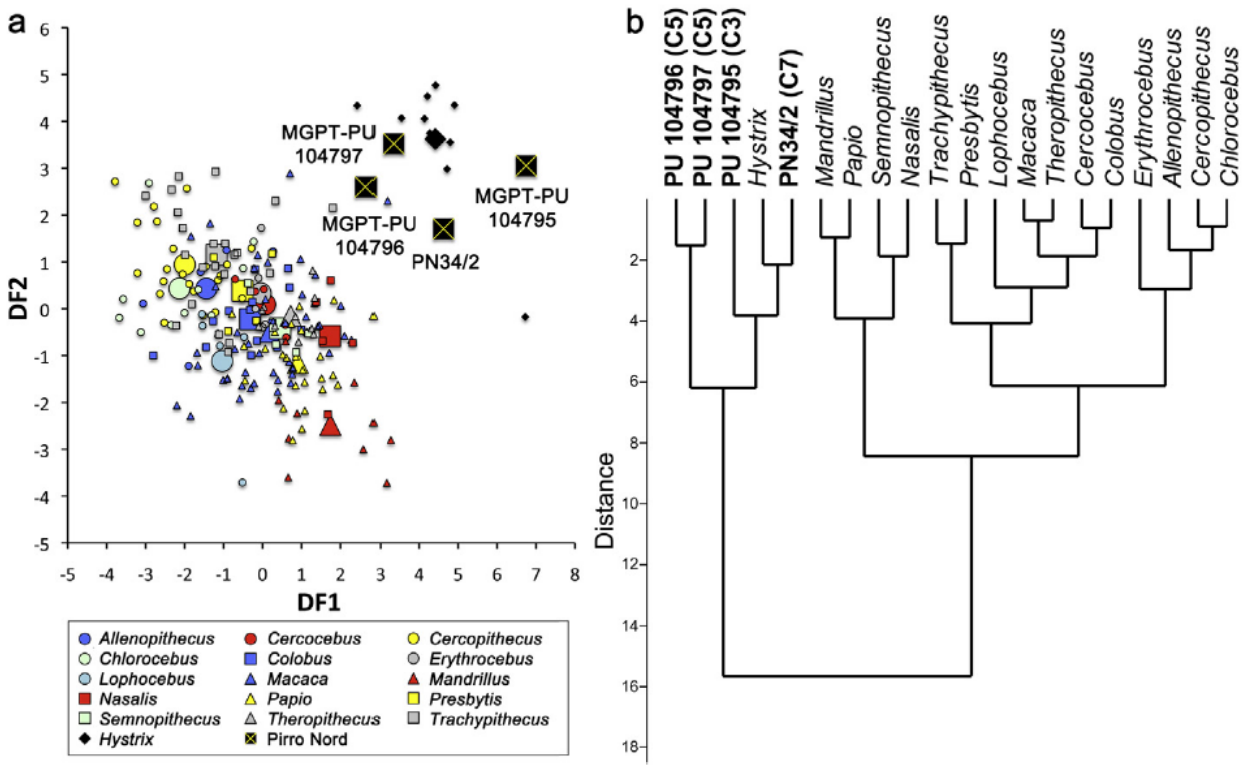

Figure 9. Results of the discriminant analyses based on Mosimann shape variables for C3eC7 cervical vertebrae of extant cercopithecids and porcupines, further showing the morphometric affinities of the most complete Pirro Nord vertebrae (including one of those previously published, and here identified as a C7). a. Bivariate plot of the first two discriminant functions. b. Cluster analysis based on extant genus centroids and the discriminant scores of the fossil specimens for all the discriminant functions (Table 2).